Phase Composition of Diffusion Zone and Shape Memory Effect in Nickelide Titanium after Ion Nitriding[1]

V.N. Timkin, V.N. Grishkov, and A.I. Lotkov

ISPMS SB RAS, 2/1, Academichesky ave., Tomsk, 634021, Russia
Phone: +7(3822) 28-69-82, Fax: +7(3822) 49-25-76, E-mail: timk@ispms.tsc.ru

Abstract – The experimental results about the structure of diffusion zone (DZ) forming in equiatomic TiNi during the ion nitriding in ammonia atmosphere at 1073 K are presented. The TiNi alloy has the B19′ monoclinic structure in initial state at 300 K. Three subzones were found in DZ of nitrided samples. The 1st subzone contains the δ-TiN compound only. The 2nd subzone has the structure of hard alloy based on the δ-TiN and Ti_4Ni_2N nitridic phases surrounded by the cubic B2-TiNi matrix. The 3rd subzone is characterized by the next sequence of phase composition: B2-TiNi + Ti_4Ni_2N → → B2–TiNi → B2 + B19′ → B19′. The chemical composition and the martensitic transformations of B2 phase in depend on the distance from δ-TiN layer was studied. The formation of stress-induced martensitic phases was found in DZ under tension and torsion of nitrided samples. The regularities of shape recovery in nitrided TiNi under subsequent heating were established. It was shown that the nitrided TiNi may be used practically as shape memory alloy.

1. Introduction

It is well known that the TiNi based alloys demonstrate high wear and corrosion resistance and high strength properties. Nevertheless, the recent results have shown that the exchange of chemical components between alloys and external medium took place [1]. The traditional way how to improve the strength and corrosion resistance is the formation of protective surface coatings. We choose the ion nitriding in glow discharge plasma for the synthesis of δ-TiN coating on the surface of equiatomic TiNi. Up to now, there are no data about the application of this method for TiNi based alloys.

The effect of ion nitriding and following loading on phase composition in surface layers of equiatomic TiNi and the shape memory effect (SME) in nitrided samples are shortly presented.

2. Materials and methods

The TiNi alloy (50.1–50.2 at % Ni) was prepared from titanium iodide and electrolytic "H–0" nickel by electric arc melting with sixfold remelting. The rolled sheets and wire were manufactured out of which the experimental samples were taken. The ion nitriding was carried at 1073 K in ammonia atmosphere. X-ray phase analysis was performed using the method of successive chemical removing of surface layers and by scanning of immovable samples with successive change of an angle between incident X-ray beam and sample surface. The X-ray diffractometer was equipped with thermal attachment for testing of transformation temperatures. The chemical composition of B2 phase was estimated with the precision about ± 0.2 at % Ni using a calibration dependence of the unit cell as a function of Ni content [2]. Tension experiments were performed at 300 K. A television optical system was used to determine the microstructural changes under tension. The shape memory effect was studied in torsion.

3. Phase composition in nitrided TiNi

The external surface of nitrided TiNi has a uniform yellow color after short-time nitriding (< 1 h). The surface color changes to the saturated yellow with a red hue after the more prolonged nitriding. Only δ-TiN mononitride was found in the external surface layer by X-ray diffraction. Based on data of above-mentioned X-ray methods, the distribution of phases in depend on a distance from external surface (L) are presented in Fig. 1.

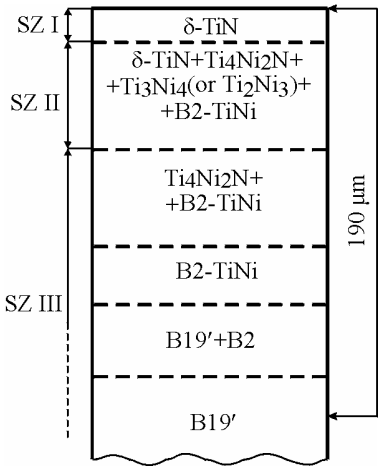

Fig. 1. The distribution of phase composition in DZ of samples, nitrided at 1073 K (4 h)

[1]The work was supported by the Based Research Program of SB RAS (2007–2009, Project No. 3.6.2.2) and Complex Integrative Project of SB RAS (2007–2009, Project No. 2.3).

The boundaries between subzones (SZ) in a DZ are very weakly expressed. Their positions are noted conditionally. The B2 phase volume fraction (VF) increases as function of L approximately to the middle of III SZ and one decreases again in a lower part of III SZ where two-phase field B2 + B19′ is observed. The appearance of B2 phase at 300 K is connected with the complicated redistribution of Ti and Ni atoms in DZ during the formation of a δ-TiN layer at 1073 K. It is confirmed by an evaluation of a B2 phase chemical composition using X-ray method. It can be seen from Fig. 2 that B2 phase Ni content decreases quickly from maximal value near the δ-TiN layer to the Ni concentration in initial alloy near the lower boundary of DZ.

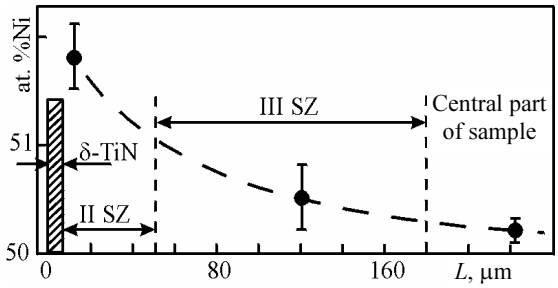

Fig. 2. B2 phase chemical composition in DZ as function of L in samples, nitrided at 1073 K (4 h)

The B2 → B19′ martensitic transformation (MT) begins in this area already at cooling from 1073 to 300 K after a nitriding finish, Fig. 3.

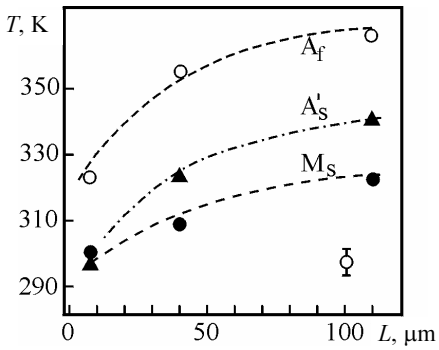

Fig. 3. The start (A'_S, M_S) and finish (A_f) temperature of MT at heating (A'_S, A_f) and cooling (M_S) in depend on L in samples nitrided at 1073 K (1 h)

But the M_f temperature (the transformation finish) is lower then 300 K. For this reason the two phase composition (B2 + B19′) will be observed in some sublayer near the lower part of III SZ in samples after long-time nitriding. This two-phase sublayer is situated not far from a δ-TiN layer in samples after a shot-time nitriding. The B2 → B19′ transformation is fully suppressed at temperatures above 300 K in the upper part of II SZ with a maximal supersaturation by Ni. The width of this sublayer increases with increasing of nitriding duration.

4. The deformation behavior of nitrided TiNi

The σ–ε tension curves for the initial and nitrided samples are presented in Fig. 4.

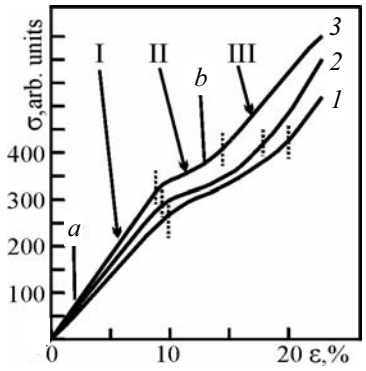

Fig. 4. The σ–ε curves for initial (*1*) and nitrided (*2* and *3*) alloys: *2* – 1; *3* – 4 h

It is seen that the hardening effect is clearly expressed after the long-time nitriding. All dependencies are typical for near equiatomic TiNi alloys: the linear ε growth with σ increasing (the I stage), the accumulation of inelastic deformation ε under small σ changes on the stage of reorientation of the initial thermal B19′ martensite (the II stage) and quasielastic and plastic deformations on the III stage. Namely, the II deformation stage is very interesting for our purposes in nitrided TiNi as a material with the shape memory.

The cross section of DZ in samples nitrided 4 h is presented in Fig. 5 under the different stresses.

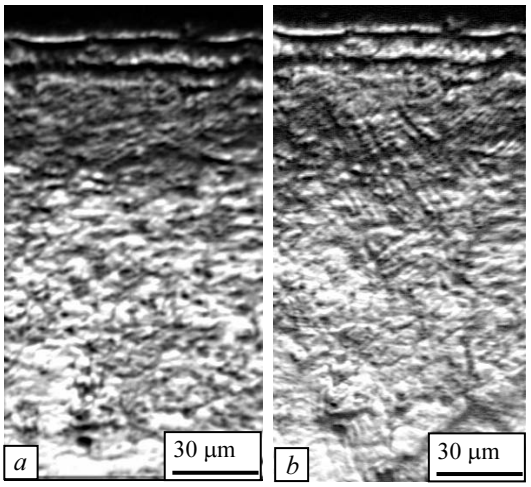

Fig. 5. Microstructure changes in DZ under tension. The ion nitriding during 4 h, 1073 K. Figs. 5, *a* and *b* correspond to *a* and *b* points in Fig. 4

The dark field under the sample surface (the upper light line) includes I SZ, II SZ and the upper part of III SZ. The lower side in Fig. 5 corresponds to the lower boundary between III SZ and the central part (the B19′ phase). The martensitic crystals have a rod-like morphology. Ones are united into the line-like structures

with its orientations along the σ direction on this deformation stage, Fig. 5, *a*. Packets are mainly orientated both along the σ direction and under angles ± 45° to it. The small packets of the fine dispersive martensite are seen in the upper part of III SZ and the lower part of II SZ to the end of the II stage, Fig. 5, *b*. We found no evidences about the growth of stress-induced R martensite under isothermal tension by "*in situ*" optical experiments. The changes of microstructure relief due to this transformation are very small and invisible by optical microscopy. But the reversible growth and the following disappearing of R phase was observed in upper part of II SZ by X-ray "*in situ*" experiments using loading and following unloading of nitrided samples in the specially equipped chamber for isothermal torsion testing, Figs. 6 and 7. (It mans that a superelastic behavior of II SZ under deformation may be caused by this transformation.)

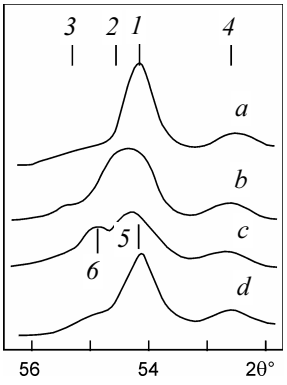

Fig. 6. The X-ray scattering near (110) B2-TiNi (*1* – (110) B2-TiNi; *2* – (200) δ-TiNi; *3* – (004) $TiNi_3$ and (221) Ti_3Ni_4; *4* – (333) Ti_4Ni_2N; *5* – (112) *R*-TiNi; *6* – (003) *R*-TiNi) depend on torsion deformation: γ = 0 (*a*); 4.2 (*b*); 10.3 (*c*); 6.3% after unloading (*d*)

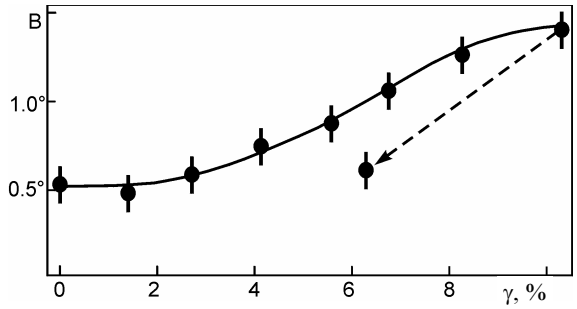

Fig. 7. The influence of deformation on half-width of (110) B2–TiNi and doublet of (300)–(112)R martensite profile (1073 K, 1 h)

Thus, it is most probable that the sequence B2 → R → B19′ MT take place in III SZ and lower part of II SZ under tension. The effects connected with a plastic deformation (the III stage and so on) are not presented in this report because ones exert the negative influence on the shape recovery in SME materials.

The problems connected with the deformation of δ-TiN layer are very important for nitrided alloys due to the weak plasticity of δ-TiN under tension. The first isolated microcracks (MC) have been observed in the surface of δ-TiN layer by the optical microscopy to the end of I stage only, Fig. 8.

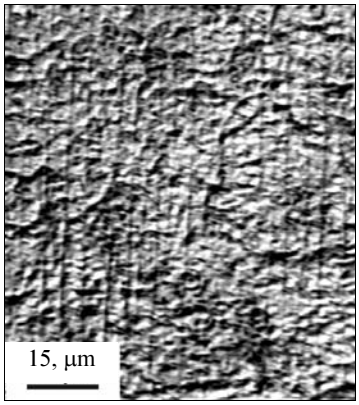

Fig. 8. Microcracks in δ-TiN layer under tension stress, corresponding to the end of II deformation stage

The MC are very narrow (about 1–2 μm) and its length are about 50–100 μm in depend on the nitriding duration. We did not observe the long MC crossing the sample surface from one to another sides. The quasiperiodic systems of MC appear on the II stage. The MC are localized in fragments. The fragment dimensions are about 50–100 μm and ≤ 200 μm after the nitriding duration 1 and 4 h, correspondingly. The MC are orientated along the perpendicular to σ direction or under angles ± 45° to one. The MC depth is limited by the δ-TiN thickness, Fig. 9.

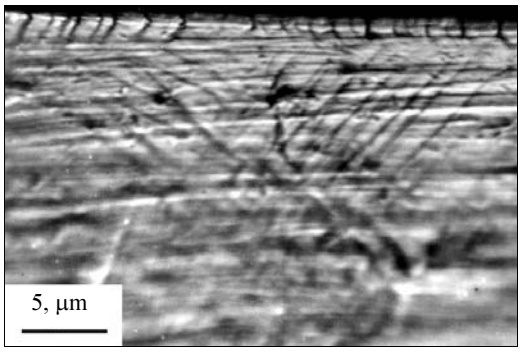

Fig. 9. Microstructure in II SZ near microcracks in δ-TiN layer (1 h, 1073 K). After sample disruption under tension

These MC are active stress in II SZ with the structure of a hard alloy. The traces of microplastic creep are clearly observed in the vicinity of MC., Fig. 9. This area is limited by the thickness of II SZ. The stress fields around MC take part in formation of stress-induced martensitic phases (R or B19′). But details of this process are unknown now.

In spite of the formation of MC we did not observe the breaking of δ-TiN particles from surfaces of nitrided samples both to the end of II stage and in sample disrupted under tension or torsion. It is a good sign for the conservation of shielding properties of δ-TiN

layer in deformed samples. But the SME was studied in nitrided TiNi in first turn.

5. Shape memory effect in nitrided TiNi

The SME were studied by the torsion of cylindrical samples, which had been deformed at 300 K under constant maximal stress (τ_{max} = 600 MPa) independently of nitriding duration, Fig. 10.

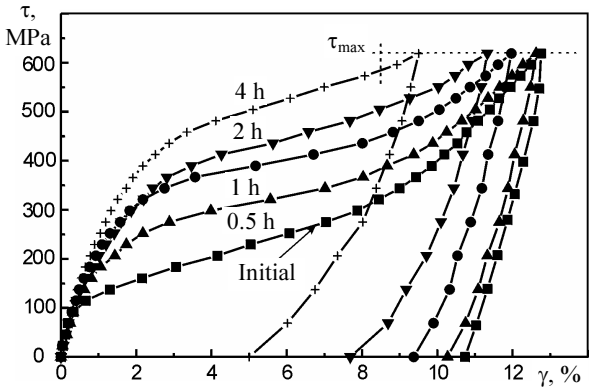

Fig. 10. The accumulation and recovery of deformation at isothermal loading and following unloading at torsion of nitrided TiNi

The γ_{max} deformation value accumulated under τ_{max} stress decreases from 12% to 11 and 9% when the nitriding duration increases to 2 and 4 h, correspondingly, Fig. 10.

The $\Delta\gamma_{un}$ value (part of the γ_{max} deformation recovers during the unloading) increases with the increasing of nitriding duration and one includes the superelasticity effect due to the formation of stress-induced R and B19′ phases inside DZ and its following disappearing under unloading. For example, the γ_{ac} value (which accumulated after unloading) decreases from 11% (in non-nitrided alloy) to 9.3, 8.0, and 5.3% in samples nitrided during 1, 2 and 4 h, correspondingly.

The shape recovery takes place at heating through the thermal range of reverse MT, Fig. 11.

The start temperature of shape recovery decreases from 320 K (in non-nitrided alloy) to 300 K (in samples nitrided 4 h). But the finish temperature of shape recovery (A_f) becomes approximately constant for all samples. The small residual plastic strain was observed after shape recovery finish. The γ_r changes vs. the nitriding duration follow the curve with maximum. The residual plastic strain values growth from 0.55% (in non-nitrided alloys) to maximal value about 1% in samples nitrided 1 h with the following linear decreasing to 0.55% after long-time nitriding (4 h). Thus, the nitrided TiNi demonstrates the enough high parameters of shape memory for practical applications.

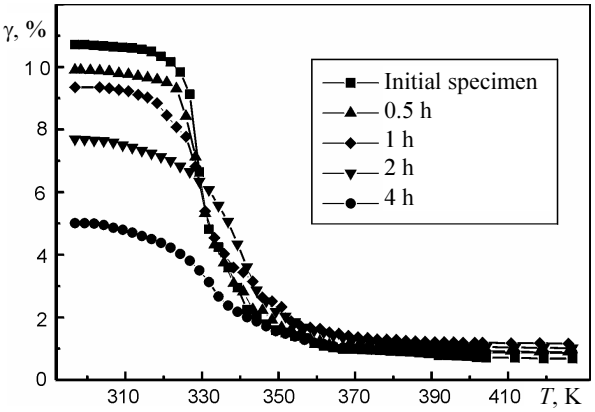

Fig. 11. The influence of nitriding duration on deformation recovery at heating through the thermal range of reverse MT

6. Conclusions

We have no possibility to discus now the physical and chemical processes, which determine the DZ structure. But few moments, which are important for further studying of nitrided TiNi, must to be marked.

The δ-TiNi layer is strongly bound with the next II SZ. No breaking of δ-TiN particles was found under torsion or tension of nitrided samples.

The phase composition changes smoothly through cross section of DZ without sharply expressed interlayer boundaries as possible stress concentrators under loading.

The B2 phases localized in DZ can be transformed into *R* or B19′ phases at cooling below 300 K or under external loading. The similar DZ can be characterized by high damping properties.

The characteristics of SME are less in nitrided samples then ones in initial alloy. But the absolute value of shape recovery is about 5–8%. It is enough for successful applications of nitrided TiNi.

References

[1] S.A. Shabalowskaya, *in Proc. Int. Conf on Martensitic Transformations "ICOMAT-95"*, Lauzanne, Switzerland, Aug. 25–28 1995, J. de Phys. IV. Coll. C8. Suppl. J. de Phys. III. 1995. Vol. 5, No. 12, pp. C8-1199–C8-1204.

[2] V.N. Grishkov and A.I. Lotkov, Physics of Metals and Metallography **50**/2, 351–355 (1985).